

Profound 2-D amplification effects for sites with soft soil underlying stiff soil

J.X. Zhao¹ and Jian Zhang²

¹ GNS Science, Lower Hutt, New Zealand, Email: j.zhao@gns.cri.nz

² Xinan Jiaotong University, Chengdu, Shichun, China

ABSTRACT :

For a 30m deep 1-D soil site of about 0.5s period with a soft soil layer at the surface overlying a stiff layer above bedrock, the short-period amplification characteristics are similar to those of the 1-D model with a single soft soil layer, in that the cross-over point separating the amplification and deamplification range is about 0.3-0.5g for peak ground accelerations (PGA). However, for a soil site with a soft layer between a stiff surface layer and the underlying bedrock, the short-period amplification ratios are drastically reduced from those of a site with a uniform soft soil layer or a site with a soft soil layer at the surface, with a cross-over point for PGA amplification ratios as small as 0.1-0.2g, depending on the thickness of the stiff soil layer. Significant differences between these two 1-D models are observed at periods up to 1.0s. We investigate the 2-D effect from a 2-D soil basin with identical vertical shear-wave velocity profile at the basin center to that of the 1-D model. We model six 2-D trapezoidal basins that have a symmetric soil/bed rock interface with width/depth ratios of 3, 6, and 10, subjected to a suite of rock site records. For the first set of three basins, the soft soil layer is over the stiff soil, while the second set has a soft soil layer between the stiff layer and the bedrock. We find that the differences in response spectral amplification ratios between the two sets of basins are reduced from those of the two 1-D models, and show profound 2-D effects.

KEYWORDS: Basin effect, soil site amplification

1. INTRODUCTION

Earthquake ground motions are often amplified by soft soil layers and the amplification can cause significant structural damage. Much research has been done in assessing soil amplification effect (Kawase and Aki 1989). In many engineering applications, 1-dimensional (1-D) equivalent linear or fully nonlinear methods are used (Idriss 1990). For soft soil basins, 2- and 3-D nonlinear modeling is occasionally used (Joyner 1975). In the amplification curve for peak ground acceleration (PGA), the cross-over point that separates the amplification from the deamplification ranges of the rock site PGA, is assumed to vary typically between 0.3-0.5g, because of the limited shear strength of the soft soil. However, for a site with a layer of soft soil and a layer of stiff soil subjected to earthquake ground shaking, amplification ratios differ significantly for a case where the soft soil layer is beneath a stiff soil layer from a case where the soft soil layer is at the site surface. In the present study, we use 10 soil site models, four 1-D models and six 2-D models, to investigate this aspect. The first 1-D model has a layer of 30m soft soil (with a shear-wave velocity of 175m/s) over a layer of 48m weak rock with a shear-wave velocity of 750m/s on an engineering bedrock half space with a shear-wave velocity of 1000m/s. The second 1-D model has a soil layer 16m of the same soft soil over the weak rock layer and the engineering bedrock. For the other two 1-D models, the 30m soils are divided into two layers, each having a thickness of 16m (top layer) and 14m (2nd layer), with the soft soil (weak) layer being over or underneath a stiff soil layer with a shear-wave velocity of 350m/s (stiff). The last 1-D model has a layer of soft soil of 16m over a layer of weak rock above the engineering bedrock. Figure 1(a) shows the geometry of the 2-D basins, which all have a soil layer of 30m at the centre. The slope of the boundary at each horizontal side is 45 degrees, with a length/depth ratio of 10, 6 and 3. In the two horizontal sides of the basin model vertical energy transmitting boundaries (viscous dashpots) are located at a distance of 180m from the basin edge and a layer of weak rock is used between the basin bottom and the horizontal energy transmitting boundary. The use of this weak rock layer also aims at reducing the effect of reflected waves by the vertical energy transmitting boundaries on the basin response, and our tests show that a 180m distance is large enough to minimize the effect. For both 1-D and 2-D cases, the models with a soft (weak) soil layer at surface (over a stiff soil layer) is labeled as WS and the model with a stiff soil layer at the surface (over a weak soil layer) as SW. Both 1-D and 2-D models are

assumed to be subjected to SH waves (out-of-plane in shear). Figure 1(b) shows the soil shear-modulus reduction curve used for all models.

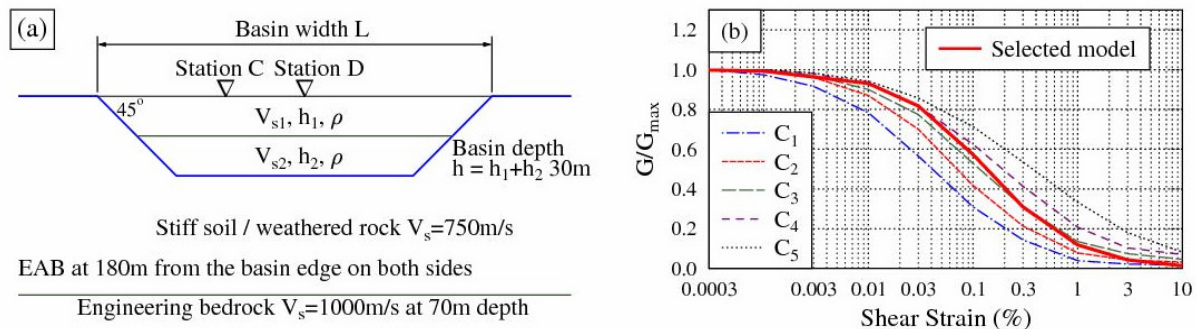


Figure 1 2-D model geometry in (a) and reduction curves for soil shear modulus in (b). Energy absorption boundaries (EAB) are placed at 180m from the basin edges and at a horizontal EAB at a depth of 70m.

2. STRONG MOTION RECORDS

We selected 98 rock site (NEHRP site class A/B (BSSC, 2000) records obtained from shallow crustal earthquakes. In order to derive a reliable mean amplification curve, we need to have a reasonably large number of records with a suitable range of excitation spectra to constrain the mean amplification curve at the weak and strong ends of the excitation spectra. A problem with using small records is that they increase the overall variability of the amplification ratios, while the amplification ratios from low-amplitude records are not relevant to engineering applications. Zhao et al (1999) find that the amplification ratio of a scaled record does not introduce additional variability, and so we scaled some of the selected records with PGA less than 0.01g by a factor of 0.2, representing ground motions either at a remote site from a large event or at short distance from a small event. To compensate for the lack of very strong rock site records, some records with PGA greater than 0.2g were scaled by a factor of 2 representing strong ground motions from very large earthquakes.

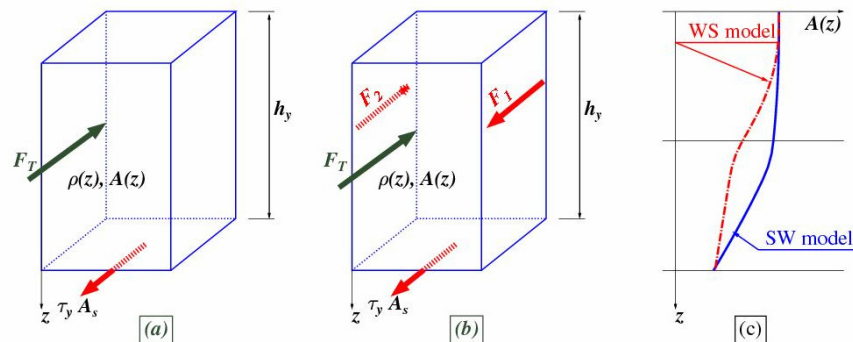


Figure 2 Equilibrium of a soil element with a finite size. Not that the bottom horizontal line in (c) is at the total basin depth and the bottom surface in (a) and (b) is the depth of soil yielding

3. MAXIMUM PEAK GROUND ACCELERATIONS FOR A SOIL SITE

Soft soil sites tend to limit the maximum peak ground accelerations because of the shear strength of the soil. However, this aspect is not well understood, especially the combined effect of the soil yielding stress and the thickness of the soil layer. Figure 2 illustrates the equilibrium of a soil element between the soil site surface and the horizontal surface where soil reaches the yielding stress for 1-D and 2-D models. Figure 2(c) presents a possible acceleration distribution $A(z)$ along depth z (similar to 1.0 + the first modal shape) for two 1-D soil models subjected to SH wave before soil reaches the yielding stress. WS in Figure 2(c) stands for the 1-D model with a soft soil layer at the surface and SW stands for the 1-D model with a stiff soil layer at the surface. F_T is the total inertial force of the soil element. For a 1-D model, the shear-stress reaches the yielding value τ_y

(this would be the maximum shear stress that the soil can produce for an elasto-perfectly-plastic nonlinear model) at a depth h_y , and at a given time (when the surface acceleration reaches PGA), the PGA at the ground surface can be computed by

$$\tau_y = F_T = \int_0^{h_y} \rho(z) \ddot{u}_T(z) dz \quad \ddot{u}_T(z) = \text{PGA} \times A(z) \quad \text{PGA} = \frac{\tau_y}{h_y \rho_w} \quad \rho_w = \frac{1}{h_y} \int_0^{h_y} \rho(z) A(z) dz \quad (1,a,b,c,d)$$

where $\rho(z)$ is the mass density, $\ddot{u}_T(z) = \text{PGA} \times A(z)$ is the total acceleration of the soil at a depth z and ρ_w is the weighted mass density. The area for the cross section A_s in Figure 2 is assumed to be 1.0. Note that $A(z) = 1$ at $z=0$ and yielding would always occur in the soft soil layer because of large shear-strain (derivative of the modal shape with respect to depth) and small yielding stress of the soft soil. For a stiff soil layer over a soft soil layer, soil yielding occurs in the soft soil layer and the acceleration distribution in the stiff soil layer can be close to constant. In this case, h_y is always larger than the thickness of the stiff soil layer and ρ_w is very close to the average mass density of the stiff soil layer. PGA is then proportional to τ_y/h_y (and to the thickness of the stiff soil layer). For a case of a soft soil layer over a stiff soil layer, h_y will be generally smaller than the thickness of the soft layer for the 1-D model investigated in the present study. The weighted mass density ρ_w is generally less than the average density of the soft soil layer in the SW model, because $A(z)$ decreases quickly from 1.0 at the soil surface with increasing depth in the soft soil layer. The combined effect of small weighted mass density and h_y in the WS 1-D model, the PGA derived from Equation 2(c) is likely to be considerably larger than that from the SW mode, even if the soil yielding stresses for the soft soil layers are the same for the two models. This would also apply to a 1-D model with a uniform layer of soft soil. For a site with a thin layer of soft soil, the depth where the soil yields is generally smaller than that of a site with a thick soft soil, leading to a larger PGA at the ground surface for the shallow soil site than for a deep soil site.

For a 2-D basin, the effect of the soft soil layer will be modified by the basin geometry in two aspects: the basin has a much reduced radiation damping compared with for a 1-D model, because of the reflection from the boundary at each side of the basin, leading to much larger amplification ratios than in a 1-D model at weak ground shaking when viscous material damping is neglected as in the computer code used in the present study. The lateral boundaries also provide constraint for the shear deformation within the soil basin and limit the amount of shear strain developed in the soil. This restraint effect is illustrated by the two resultant forces applied to a soil element in Figure 2(b). Following the equilibrium of the soil element in Figure 2(b), the following solutions can be obtained, assuming that the soil element has a unit thickness and a unit area of cross section,

$$F_1 = \int_0^{h_y} \tau_1(z) dz \quad F_2 = \int_0^{h_y} \tau_2(z) dz \quad \text{PGA} = \frac{\tau_y + F_1 - F_2}{h_y \rho_w} \quad (2a,b,c)$$

where $\tau_1(z)$ is the shear stress acting on the right hand side of the soil element and $\tau_2(z)$ is the shear stress acting on the left hand side. For a symmetric mode across the ground surface of a symmetric basin, $F_2 = -F_1$ if the soil element is cut at the centre of the basin, but this is not necessarily the case for an arbitrary vertical element cut from an arbitrary basin geometry. At the centre of a symmetric basin, the amplitude of shear stress $\tau_1(z)$ and $\tau_2(z)$ generally decreases with increasing basin length and is negligible if the L/h (length/depth ratio) is over 16, when the 2-D effect is very small. If the soil element is at the left half of a symmetric basin, the resultant force $F_1 - F_2$ is positive and $F_1 - F_2$ is also positive at the right half of the basin when the basin deforms in a symmetric manner. Equation (2) conceptually suggests that the PGA of a 2-D symmetric basin may generally increase with the increasing distance from the basin centre, and the PGA at the basin centre would generally increase with decreasing basin L/h ratio. However, at a station close to the basin edge, PGA is no longer associated with the symmetric mode and Equation (2c) breaks down. The PGA at the centre of a 2-D basin may not always be larger than that of a 1-D model with identical vertical shear-wave profile, as the yielding depth for a 2-D model may differ significantly from that of a 1-D model.

4. PGA AMPLIFICATION RATIOS

The amplification ratios are fitted by the following equations,

$$\ln(A_R) = \ln(A_{\max}) \frac{\ln(Y_R + c) - \ln(Y_{\text{cross}} + c)}{\ln(c) - \ln(Y_{\text{cross}} + c)} \quad (3)$$

where A_R is the response spectral amplification ratio, A_{\max} is the maximum amplification ratio at small soil shear-strain (elastic response), Y_R is the response spectrum of a rock site record, Y_{cross} is the cross-over point that separates the amplification from the deamplification range (i.e. $A_R = 1.0$ when $Y_R = Y_{\text{cross}}$) and c is a constant that controls how rapid is the reduction in amplification ratio with increasing rock site spectra. We also used more complicated equations for 0.5s period of the 2-D models, as the simple form of Equation (3) cannot be fitted the amplification ratios very well.

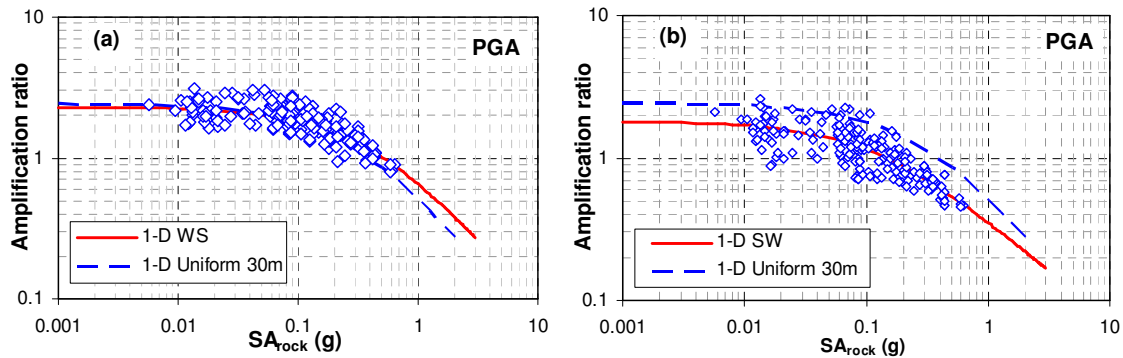


Figure 3 PGA amplification ratios for three 1-D models, (a) a soft soil layer over a stiff soil layer; and (b) a soft soil layer underneath a stiff soil layer, together with the 1-D model with a 30m soft soil layer. The scatter for SW model is larger than that of the WS model.

Figure 3 shows the fitted PGA amplification ratios for three 1-D models, and the ratios from each record. The amplification ratios for a site with a soft soil layer at the surface (WS with $Y_{\text{cross}} = 0.47\text{g}$) are generally similar to those of the site with a uniform shear-wave velocity (with $Y_{\text{cross}} = 0.37\text{g}$). The SW mode, however, has an A_{\max} of 1.8 and a cross-over point of only 0.15g, much smaller than those of WS model, consistent with the conceptual illustration presented in Section 3. The 1-D model of 30m soil with a uniform shear-wave velocity of 175m/s has an $A_{\max} = 2.3$ (very similar to the 1-D WS model) and $Y_{\text{cross}} = 0.47\text{g}$ (much larger than that of the 1-D SW model, see Table 1). The scatter for the SW model is larger than that for WS model, presumably because of the different scatter in the rock site spectra at different spectral periods.

Table 1 Maximum amplification ratio and cross-over points for four 1-D models

Model names	PGA			At site natural period			Site natural period (s)
	A_{\max}	Y_{cross} (g)	c	A_{\max}	Y_{cross} (g)	c	
1-D Uniform 30m	2.45	0.37	0.25	4.2	0.7	0.15	0.72
1-D uniform 16m	2.35	0.51	0.39	3.5	1.45	0.4	0.37
1-D WS	2.35	0.47	0.56	3.6	1.15	0.42	0.47
1-D SW	1.8	0.15	0.12	3.4	0.42	0.11	0.68

Table 1 shows the parameters for amplification ratios of four 1-D models at PGA and the site natural periods, and Figure 4 shows the corresponding amplification ratios. At weak PGA excitation, the amplification ratios for the first three 1-D models in Table 1 are almost identical with A_{\max} being about 2.4, while the SW model has an A_{\max} of only 1.8. The PGA cross-over point is 0.51g for the 1-D 16m model and reduces to 0.37g for the 30m deep uniform model. At large excitation PGA, the amplification ratios for the 16m uniform model are larger than those of the 30m model, consistent with those illustrated by Equation 1, i.e., for the shallow model, h_y is likely to be smaller than that of the deep model, leading to a larger PGA at the ground surface than that for the deep model.

The maximum amplification ratio is usually at a spectral period somewhere over the elastic natural period of a soil site, and the amplification ratios at the site natural periods would provide some indication for the peak

amplification ratios. Table 1 shows the parameters for the amplification ratios for four 1-D models and Figure 4(b) shows the corresponding amplification ratios. Under weak excitation spectra, the amplification ratios at the site natural periods are very similar for all four models, as expected, because, if the site soil has identical material and radiation damping ratios, the Fourier spectral amplification ratios for the four 1-D models will be identical at the site natural period, leading to similar response spectral ratios when the soil responds elastically. The amplification ratios for the SW model are much smaller than those of the other models for a rock site spectrum over 0.01g. The cross-over point varies from 0.7g for the 30m uniform model to 1.45g for the 16m uniform model while the 1-D WS model has a cross-over point of 1.15g. Similar to PGA, the cross-over point for the SW model is much smaller than those of the other models, only 0.42g.

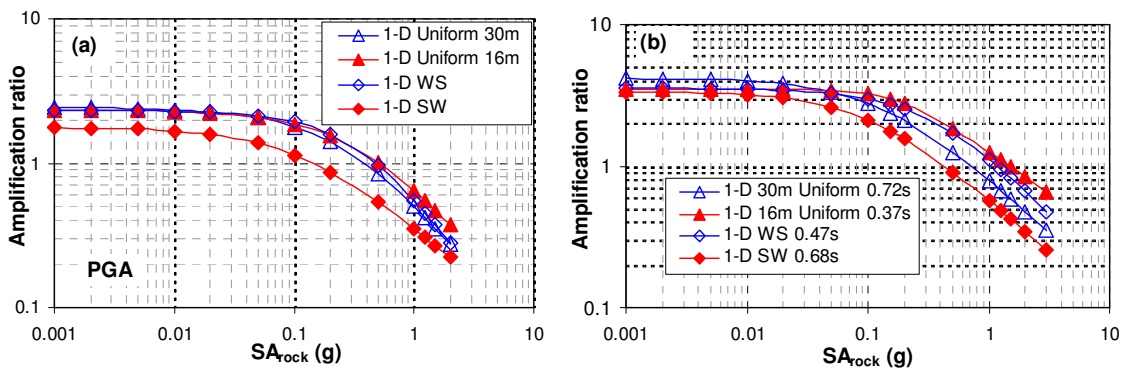


Figure 4 Amplification ratios for four 1-D and models at (a) PGA, and (b) at site elastic natural periods

Figure 5 shows the PGA amplification ratios for two 1-D models, and two 2-D models with an L/h ratio of 10. The amplification ratios at small excitation PGA for the 2-D models at both stations C and D are much larger than those for the corresponding 1-D models. The difference between amplification ratios for the 1-D and 2-D WS models decreases quickly with increasing excitation PGA, leading to very similar amplification ratios between the two models at moderate and large excitation PGA at both stations C and D. The amplification ratios for the 2-D SW model are, however, are considerably higher than those of the 1-D SW model for all levels of excitation PGA, suggesting that the 2-D effect is more profound for a site with soft soil layer underneath a stiff soil layer.

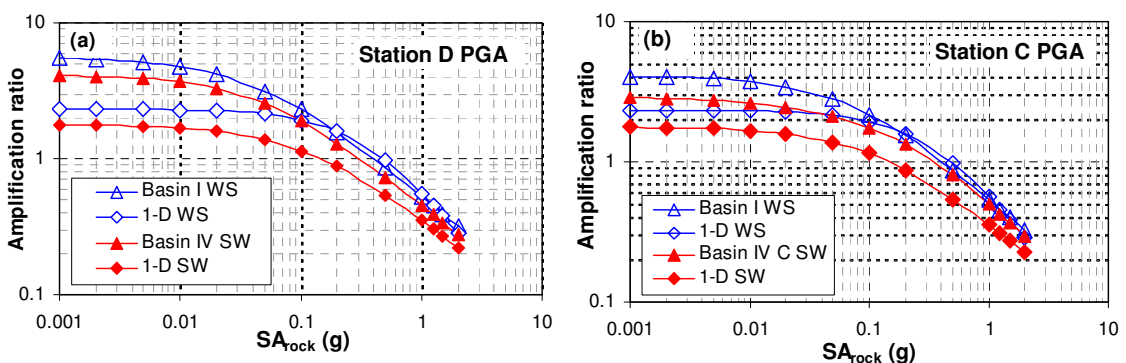


Figure 5 PGA amplification ratios for two 1-D and two 2-D models (Basins I and IV with L/h=10), (a) at station D (the basin centre) and (b) at station C as illustrated in Figure 1(a).

Table 2 shows the parameters for the amplification ratios for all 2-D models used in the present study. For the SW models, A_{max} is 4.1 for the 2-D model but is only 1.8 for the 1-D models. Among the 2-D models, A_{max} does not have a regular variation trend with basin L/h ratio. The cross-over point is about 0.3g for the 2-D SW model at station D compared with 0.15g for the 1-D SW model. The cross-over points increase with decreasing L/h ratios for both SW and WS models. The cross-over point for a basin with L/h=3 is nearly twice that for a basin with L/h=10 at station D for both SW and WS models. The differences in the cross-over points

between 2-D SW and WS models are much smaller than that between two 1-D models (SW and WS) for all cases presented in Tables 1 and 2. Similar patterns can be observed for the amplification ratios at station C.

Table 2 Maximum amplification ratio and cross-over points for six 2-D models

PGA		Station D			Station C		
		A_{max}	Y_{cross} (g)	c	A_{max}	Y_{cross} (g)	c
Basin	L/h	WS 2-D model					
I	10	5.6	0.38	0.04	4.1	0.39	0.07
II	6	6.7	0.46	0.03	4.3	0.46	0.11
III	3	6.1	0.7	0.06	4.5	0.57	0.08
Basin	L/h	SW 2-D model					
IV	10	4.1	0.3	0.05	2.9	0.34	0.12
V	6	3.9	0.35	0.09	2.5	0.48	0.16
VI	3	3.3	0.6	0.22	2.8	0.54	0.17

5. SPECTRAL AMPLIFICATION RATIOS

Figure 6 shows the amplification ratios at 0.2s spectral period. The amplification ratio at a rock spectrum less than 0.1g is 2.0 for the 1-D WS model with a cross-over point of 1.0g, and only 1.24 for the 1-D SW model with a cross-over point of 0.2g. At a 1.0g rock motion spectrum, the amplification ratio for the 1-D SW model is just over 0.5, about half of the 1-D WS models. For the 2-D WS model at station D, the amplification ratios at strong ground shaking are very similar to those of the 1-D WS model. At weak excitation, the amplification ratios for the 2-D SW are close to the 2-D WS model and are much larger than those of the 1-D SW model. For the SW models, 2-D effect enhances the amplification ratios significantly at weak and moderate ground shaking but the ratios for the 2-D SW model decrease quickly with increasing excitation spectra. The cross-over point for the 2-D SW model is about 0.45g, but only 0.2g for the 1-D SW models. At strong shaking, 2-D effect still enhances the amplification ratios of the SW model more than for the WS model. Very similar patterns can be observed at station C as shown in Figure 5(b).

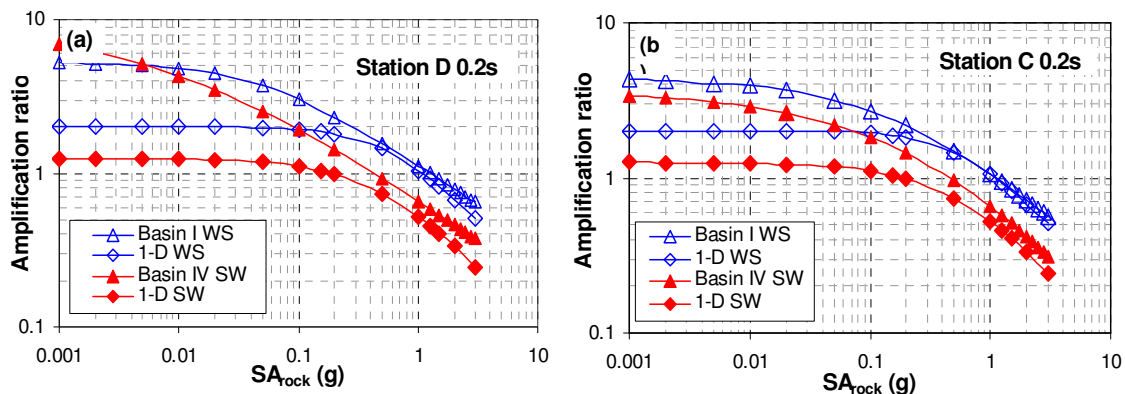


Figure 6 Amplification ratios for two 1-D and two 2-D models (L/h=10) at 0.2s spectral period, (a) at station D (the basin centre) and (b) at station C as illustrated in Figure 1(a).

Figure 7 shows the amplification ratios at 0.5s spectral period. The differences in amplification ratios between the two 1-D models are large. At small excitation spectra, the amplification ratio is over 3.0 for the 1-D WS model with a cross-over point being over 1.1g, and the ratio is only 2.0 for the 1-D SW model with a cross-over point of about 0.25g. At small excitation spectra, the amplification ratios for the two 2-D models are similar but the amplification ratios for the SW models decrease with increasing excitation spectra more rapidly than for the WS models. At excitation spectra over 0.1g, the amplification ratios are very similar for the 1-D and 2-D WS models at both stations C and D. The amplification ratios for the 2-D SW model at station D are very similar to that of the 1-D SW model at very large excitation spectra. However, at station C, the amplification ratios for

the 2-D WS model are considerably larger than those of the 1-D SW model as shown in Figure 6(b).

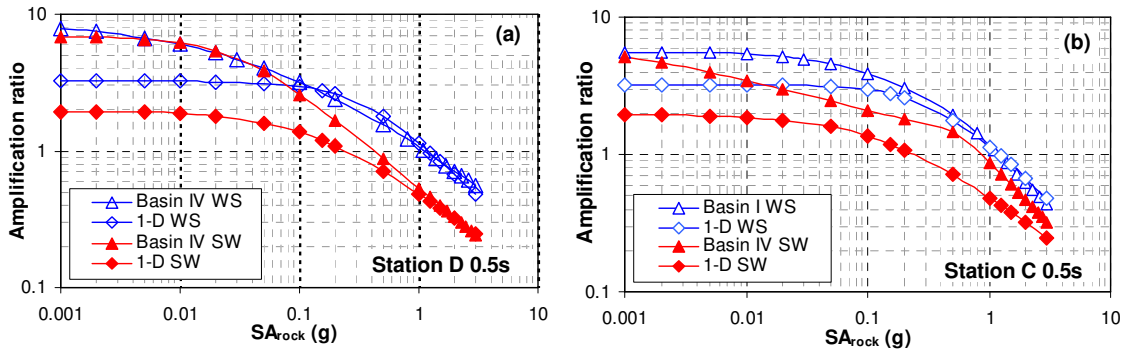


Figure 7 Amplification ratios for two 1-D and two 2-D models at a spectral period of 0.5s, (a) at station D (the basin centre) and (b) at station C as illustrated in Figure 1(a).

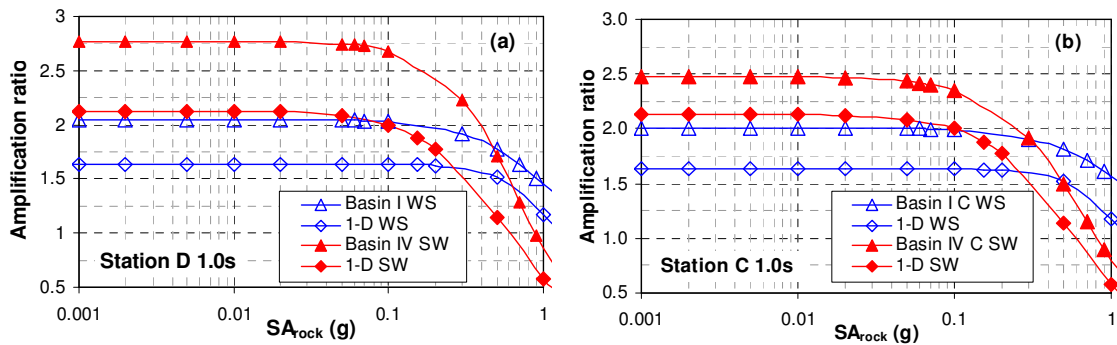


Figure 8 Amplification ratios for two 1-D and two 2-D models at a spectral period of 1.0s, (a) at station D (the basin centre) and (b) at station C as illustrated in Figure 1(a).

Figure 8 shows the response spectral amplification ratios at 1.0s spectral period. In contrast with short periods, the amplification ratios for the SW models are larger than those of WS models for both 1-D and 2-D models at stations C and D, apart from very large excitation spectra. The amplification ratios for the SW models decrease rapidly with increasing excitation spectra over 0.1g.

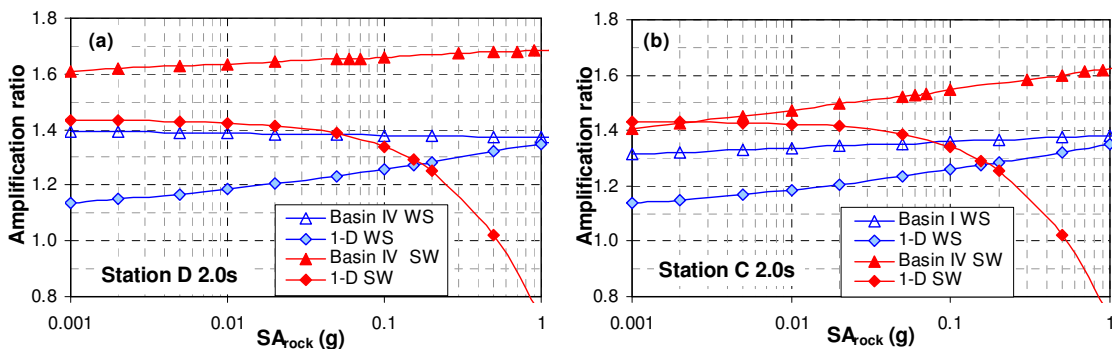


Figure 9 Amplification ratios for 2 1-D and 2 2-D models at a spectral period of 2.0s, (a) at station D (the basin centre) and (b) at station C as illustrated in Figure 1(a).

Figure 9 shows the amplification ratios at 2.0s spectral period. Only the amplification ratios for 1-D SW model show the effect of soil nonlinear response – with amplification ratios decreasing with increasing excitation spectra. For all other models, the amplification ratios are either constant or even increasing with increasing excitation spectra. Apart from the 1-D SW model at very large excitation spectra, the SW models tend to have larger amplification ratios than the WS models.

6. CONCLUSIONS

We have investigated the response spectral amplification ratios for a soil site with/without soft soil layers for both 1-D and 2-D cases. Our results suggest that the PGA at a soft soil site surface is a function of soil shear strength, the depth of the soil layers and the location of soft soil layers. For a 1-D case, the PGA at the ground surface is likely to be inversely proportional to the thickness of the soft soil layer. A shallow soft soil layer generally produces larger PGAs than a deep soft soil layer when subjected to strong ground shaking. The location of the soft soil layer also is an important factor governing the site amplification ratios. A 1-D site with a stiff soil layer over a soft soil layer tends to have very small amplification ratio for short period ground motions compared with sites that have a single soft soil layer or a soft soil layer over a stiff soil layer. The PGA cross-over point that separates amplification from deamplification ranges of the excitation spectra varies from 0.4g to 0.5g for single soft soil layer or a soft soil layer over a stiff soil layer for 1-D models and is about only 0.15g for the 1-D model with a stiff soil layer over a soft soil layer. The cross-over point at the site natural elastic periods varies between 0.7 and 1.45g 1-D models with a uniform soft soil layer with a thickness of 16-30m and a site with a soft soil layer over a stiff soil layer, and is only 0.4g for a 1-D model with a stiff soil layer over a stiff soil layer. For spectral period up 1.0s, the amplification ratios for a site with a soft soil layer below a stiff layer are all much smaller than those for the other 1-D models for all range of excitation spectra.

At weak excitation, the PGA amplification ratios for a 2-D model with a soft soil layer underneath a stiff soil layer are generally much larger than those of the corresponding 1-D models. The PGA amplification ratios for the 2-D model with a stiff soil layer over a soft soil layer at strong shaking are enhanced significantly by the 2-D effect. The cross-over point for the 2-D SW model is twice that of the 1-D SW model while the cross-over points are similar between the 1-D and 2-D WS models with $L/h=10$, suggesting profound 2-D effects for site with a soft soil layer underneath a stiff layer. At 0.2s and 0.5s spectral period, the two types of basin have similar amplification ratios at weak excitation spectra and the difference at strong excitation appears to quite large but still smaller than differences between the two types of 1-D basins. At spectral periods of 1 and 2s period, model with a soft soil layer underneath a stiff soil layer has larger amplification ratios at a wide range of excitation spectra for both 1-D and 2-D cases. At 2s spectral period, the amplification ratios of only the 1-D model with a soft soil layer beneath a stiff soil layer show soil nonlinear response, e.g. amplification ratios decrease with increasing excitation spectra.

ACKNOWLEDGEMENT

The authors would like to thank Drs. Jim Cousins and S.R. Uma for their review of the manuscript and this project is supported by Foundation for Research Science and Technology of New Zealand, Contract No. C05X0402.

REFERENCES

- Idriss IM (1990), Response of soft soil sites during earthquakes, *In: Proc. Memorial Symp. to honour Professor Harry Bolton Seed*, Berkeley California, Vol 2, 273-289.
- Joyner WB (1975), A method for calculating nonlinear seismic response in two dimensions, *Bulletin of Seism Soc of America*, 65(5): 1337-1357.
- Kawase H and Aki K (1989), A study on the response of a soft basin for incident S, P, and Rayleigh waves with special reference to the long duration observed in Mexico City, *Bulletin of the Seismological Society of America*, Oct; 79: 1361 - 1382
- Zhao JX, Davenport PN and McVerry GH (1999), Modelling and earthquake response of Gisborne Post Office site, New Zealand, *Bulletin of the New Zealand Society for Earthquake Engineering*, 1999;32(3): 146-169.
- BSSC (2000), Building Seismic Safety Council, The 2000 NEHRP Recommended Provisions for New Buildings and Other Structures, Part I (Provisions) and Part 2 (Commentary), FEMA 368/369, Washington DC